

ARTICLE OPEN

Optically invariant InGaN nanowire light-emitting diodes on flexible substrates under mechanical manipulation

Mohsen Asad^{1,2}, Renjie Wang³, Yong-Ho Ra³, Pranav Gavirneni¹, Zetian Mi^{3,4} and William S. Wong^{1,2}

The integration of GaN-based light-emitting diodes (LEDs) onto flexible platforms provides opportunities for conformal lighting, wearable electronics, and bendable displays. While this technology may enhance the functionality of the light source, the development of flexible GaN LEDs suffers from performance degradation, when mechanical bending is applied during operation. A unique approach to eliminate the degradation employs dot-in-wire structures, using cylindrical light-emitting heterostructures that protrude above the flexible platform, separating the active light-emitting region from the bending substrate. Here, we demonstrate the optical enhancement of nanowire light emitters by changing the geometric orientation within a $1 \times 1 \text{ mm}^2$ array of nanowires on a flexible platform through bending of the substrate platform. The flexible structures were achieved by transferring GaN nanowire LEDs from sapphire substrates onto flexible polyethylene terephthalate (PET) using a “paste-and-cut” integration process. The I–V characteristics of the nanowire LEDs showed negligible change after integration onto the PET, with a turn-on voltage of 2.5 V and a forward current of 400 μA at 4 V. A significant advantage for the nanowire devices on PET was demonstrated by tilting the LEDs through substrate bending that increased the electroluminescence (EL) intensity, while the I–V characteristics and the EL peak position remained constant. Through finite-element analysis and three-dimensional finite-difference time-domain modeling, it was determined that tilting the protruding devices changed the effective distance between the structures, enhancing their electromagnetic coupling to increase light output without affecting the electrical properties or peak emission wavelength of the LEDs.

npj Flexible Electronics (2019)3:16; <https://doi.org/10.1038/s41528-019-0059-z>

INTRODUCTION

GaN-based “dot-in-nanowire” light-emitting diodes (LEDs), cylindrical devices that mimic a quantum dot within a nanowire (NW) structure, are an emerging technology for phosphor-free white-lighting applications and ultraviolet light emitters.^{1,2} The emission from an array of LEDs, having a typical diameter of $\sim 250 \text{ nm}$, is dependent on waveguide modes coupled through the geometry of the cylinder and the distance between neighboring devices. Geometric modifications through altering the LED diameter and spacing enables optimal light extraction within a network. Fundamental waveguide modes are established through a fixed periodic array of LEDs that creates a quasi-two-dimensional photonic crystal.^{2–6} Integrating these light emitters onto flexible substrates would allow the LED positions to change by mechanically manipulating the flexible platform, enabling a novel approach to geometrically control the photonic devices. Earlier reports showed the integration of core/shell InGaN/GaN NW LEDs into a flexible polymeric substrate,⁷ by embedding the devices within an elastomeric layer. While creating a flexible assembly, the encapsulation of the LEDs within the elastomer limits the motion of the NWs, and the LEDs would experience mechanical strain within the active region of the device during substrate bending. In addition, these initial reports did not characterize the current–voltage (I–V) behavior of the flexible NW LEDs under mechanical strain, and the effect of substrate bending on the NW LED light-output characteristics, is not well understood.

This investigation demonstrates the feasibility and understanding of using vertical NW LED structures integrated on top of flexible substrates to separate the electrically active region of the LED from the bending platform, minimizing the performance degradation encountered in flexible planar LED structures. This novel orientation avoids common problems observed in flexible LEDs, such as peak emission wavelength shifts and decreased light output during applied mechanical stress.^{8–11} This degradation is mainly due to a strain-induced piezoelectric response affecting the active region of the LED. As bending increases, piezoelectric fields produced in the quantum wells create a measurable peak shift in the electroluminescence (EL) characteristics that affects spectral uniformity of the LEDs and degrades the performance of the light emitters for applications, such as solid-state lighting and next-generation displays. This effect is less significant for cylindrical LED structures that are oriented normal to the flexible platform. Under bending, the LED devices are free to move, since the plane of bending is outside of the active region of the NW device.¹²

RESULTS

A finite-element analysis (FEA) method was used to predict the induced strain and motion of vertically oriented NW structures on flexible platforms during substrate bending. The FEA model, based on actual structures grown by plasma-assisted molecular-beam epitaxy (PAMBE), consisted of cylindrical nanostructures having

¹Department of Electrical and Computer Engineering, University of Waterloo, Waterloo, ON N2L 3G1, Canada; ²Waterloo Institute for Nanotechnology, University of Waterloo, Waterloo, ON N2L 3G1, Canada; ³Department of Electrical and Computer Engineering, McGill University, Montreal, QC H3A 0E9, Canada; ⁴Present address: Department of Electrical and Computer Engineering, University of Michigan, Ann Arbor, MI 48109, USA
Correspondence: William S. Wong (wswong@uwaterloo.ca)

Received: 7 January 2019 Accepted: 13 June 2019

Published online: 19 August 2019

diameters of ~250-nm, separated by a 350-nm pitch positioned on a 3- μm -thick GaN film in contact with a 1- μm -thick metallic electrode bonded to a 175- μm -thick flexible polyethylene terephthalate (PET) substrate. To simulate the bending stress on the PET substrate, a bending moment M , applied along the ends of the substrate, is first determined from the Stoney equation, $M = \frac{Ed^3w}{12R}$. A bending moment of 0.0225 N-m was used for $R = 38$ mm, where d and w are the substrate thickness and width, respectively, R is the radius of curvature, and E is the elastic moduli. Figure 1 shows the stress distribution within the substrate and rod structures having a “concave-up” bending radius (bending in the direction of the light emission) of 38 mm. The FEA model shows a stress-induced strain gradient with a compressive strain of 4×10^{-4} at the surface, transitioning through the PET to a tensile strain of 6.5×10^{-4} at the backside of the substrate. The calculations show the stress within the LED structures to be nearly zero, suggesting that the active region, near the tip of a cylinder, should not experience induced piezoelectric fields during bending of the substrate that may

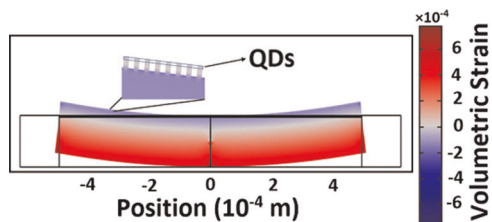


Fig. 1 The simulated strain gradient for the NW devices on PET with $R = 38$ mm. The device active region, near the tips of the nanowires, was found to be strain free. A calculated bending moment of 0.0225 N-m for $R = 38$ mm was used in the simulation

degrade the I-V characteristics and EL peak position of the light emitter.

In order to experimentally validate the simulations and confirm the bending of the flexible substrate that will not alter the optoelectronic properties of the LEDs, the integration of the cylindrical devices onto flexible platforms was achieved through a “paste-and-cut” process. The NW LEDs, grown by PAMBE, possessed a structure similar to the geometry used in the FEA model. After device fabrication, the GaN-based LEDs were bonded onto a temporary handle wafer to allow detaching the LEDs from their original sapphire process wafer.^{13–15} A laser liftoff (LLO) process enabled the transfer of the GaN-based light emitters from their sapphire growth substrate onto the flexible PET film. This approach has been effective for planar thin-film structures,^{16,17} but the integration of three-dimensional cylindrically shaped optoelectronic devices on flexible substrates has not been demonstrated.

Figure 2a–d schematically illustrates the process for the LED integration onto the PET. First, the NW LEDs are bonded with an epoxy adhesive onto a temporary receptor substrate (Fig. 2a). A 266-nm pulsed laser light, with a 5-ns pulse width, was irradiated through the transparent sapphire substrate. The laser pulse, absorbed by the GaN buffer layer, decomposes a thin region of the GaN at the GaN/sapphire interface. Following a low-temperature (40 °C) anneal to melt the decomposed interface (Fig. 2b), the GaN LED structures are detached from the sapphire substrate.¹⁴

The active region of the dot-in-wire LED is located near the tip of the cylinder structure and the transfer process positions this region at the receptor substrate surface, inverting the LEDs original orientation and reducing the extracted light. In order to return the device structure to its original orientation, a water-based silver adhesive is applied to the exposed LED back n-contact to bond the LED onto the flexible PET substrate (Fig. 2c).

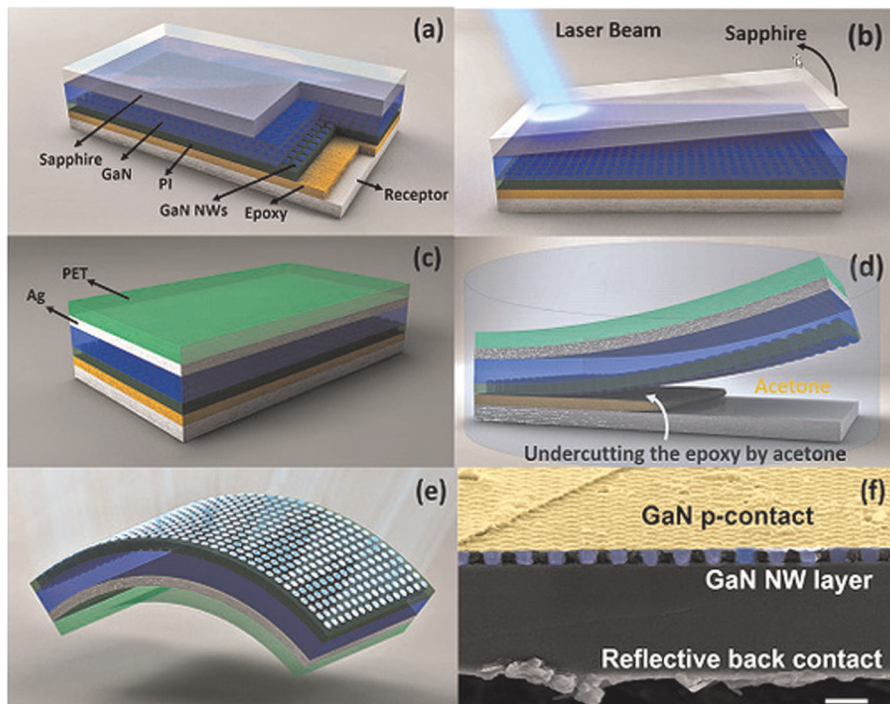


Fig. 2 Process flow of the double-transfer process. **a** The NW LED device is bonded to a temporary receptor substrate, **b** the sapphire substrate is detached from the NW devices by illuminating a pulsed 266-nm Nd:YAG laser through the sapphire to decompose the GaN at the substrate interface, **c** a metallic Ag adhesive bonds the GaN NW devices/receptor substrate structure onto a 175- μm -thick PET flexible substrate, and **d** the NW devices are transferred onto the PET by removing the epoxy bond using an acetone bath. **e** Schematic of the final transferred NW LED device on the PET substrate. **f** A cross-sectional FE-SEM image of an array of GaN NW LED devices transferred onto the flexible substrate. The gold and blue colors represent the ITO top contact and GaN NWs, respectively. Scale bar = 1 μm

Submerging the bonded structure in acetone selectively removes the epoxy bond, undercutting the LED structures and releasing the receptor substrate (Fig. 2d). The silver adhesive now serves as both the bottom n-contact and as an optical reflector to enhance light emission from the LEDs. Figure 2e schematically shows the final fabricated dot-in-wire LEDs on the flexible substrate after the two-step “double-transfer” process. Structural characterization of the LEDs after separation from its growth substrate by field-emission (FE) scanning-electron microscopy (SEM), confirmed the efficacy of the transfer process to separate the devices from their original sapphire platform onto the flexible substrate (Fig. 2f). Structural degradation to the NW device or the indium-tin oxide (ITO) p-contacts was not observed after transfer (Supplementary Fig. 1a, b). Characterization by atomic-force microscopy (AFM) also showed no observable degradation to the tip of the cylindrical LED structures after the integration process (Supplementary Fig. 1c, d).

Electrical characterization of the transferred NW LEDs supported the absence of the structural degradation observed in the FE-SEM and AFM analysis. Figure 3a shows the I–V characteristics of the LEDs biased from -5 to 5 V before and after the integration

process. A turn-on voltage of 2.5 V was measured in both cases. The I–V characteristics of the LEDs on PET shows a slight variation compared to the LEDs on sapphire; it is believed the Ag n-contact was responsible for the change.¹⁸ The Ag adhesive was not optimized for its electrical properties and was employed mainly for its use as a selective adhesive for integration onto the PET substrate. The electrical and electroluminescent measurements for the LEDs on flat and mechanically curved substrates were made using this contact; further studies are continuing to optimize the electrical contact of this bonding layer. The inset of Fig. 3a shows the blue-light emission of the NW LEDs under forward bias ($I_{\text{drive}} = 1$ mA) operating on a curved sample holder having a 38 -mm radius of curvature in a “concave-down” orientation (bending is in the direction away from the light emission).

The effect of mechanically bending the PET substrate on the LED structures was predicted to have very little stress-induced strain on the active region of the light emitter since this area is out of the plane of bending. A constant 2.5 -V turn-on voltage and an invariant forward current of 0.4 mA at 4 V were measured under different bending conditions, demonstrating that the measured electrical properties were independent of the applied bending.

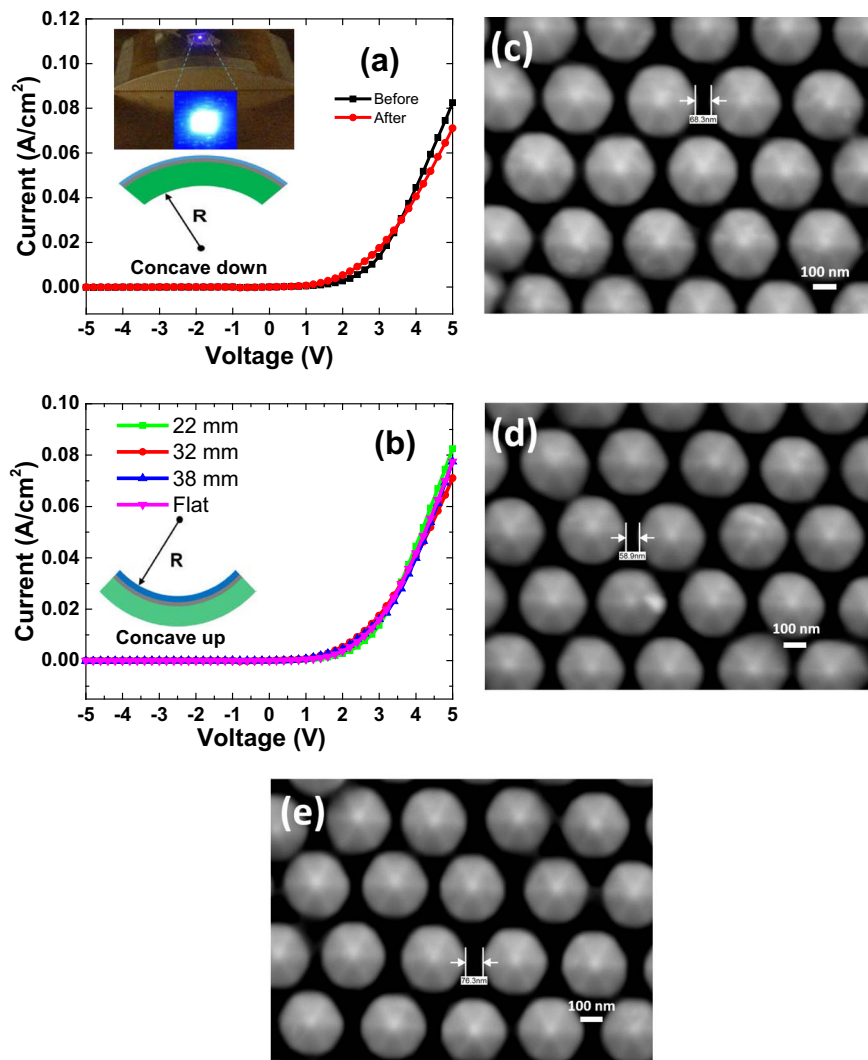


Fig. 3 **a** I–V characteristics of the NW LEDs on sapphire substrate before and after integration onto PET substrates; the slight variation in the forward current is due to the Ag contact used to bond the LEDs onto the PET. The inset shows the blue-light emission of the GaN NW LEDs operating at a 1 -mA forward current and the PET substrate flexed to a 38 -mm radius of curvature. **b** The I–V characteristics of the LEDs on PET with different concave-up bending conditions. The results show similar I–V characteristics at different radii of curvature between 22 and 38 mm. **c–e** Planview SEM images of a GaN nanowire array sample mounted on flat, 32 -mm concave-up, and 32 -mm concave-down curved substrate holder

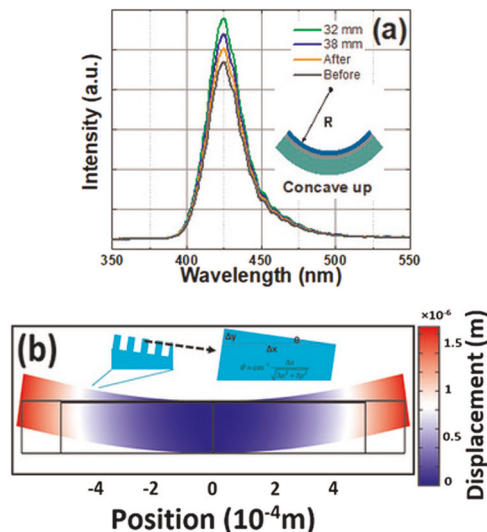


Fig. 4 **a** The measured EL spectra of the blue NW LEDs on PET before and after the double-transfer process. The transferred devices show no emission shift with different concave-up bending conditions, while the EL intensity increases with decreasing radii of curvature. **b** The displacement of the flexible devices with 38-mm concave-up radius. The tilt angles of NWs were calculated based on displacement results using $\theta = \cos^{-1} \frac{\Delta x}{\sqrt{\Delta x^2 + \Delta y^2}}$, where θ is the angle between the nanowire structure during bending after shifting in the Δx and Δy direction

The I–V characteristics of the LEDs for a substrate with a “concave-up” orientation (bending is in the direction toward the light emission) are shown in Fig. 3b for bending radii of 38, 32, and 22 mm. A measured leakage current of 10 μA at -2 V reverse bias for the flat (unbent) LEDs did not change during bending for different orientations, providing additional evidence that mechanically flexing the PET substrate does not degrade the electrical properties of the 3D GaN LED structures. The motion of the NWs was verified using SEM, with a JSM-7200F JEOL microscope, for an array of dot-in-wire structures on flexible substrates. Figure 3c–e shows the changes in the spacing between the structures for different bending orientations at $R = 32\text{ mm}$. The tip separation of the structures was measured to be 68 nm in the flat orientation, 59 nm when concave up, and 76 nm apart when concave down, showing a $\pm 8\text{--}9\text{-nm}$ range in tip separation depending on the bending direction, consistent with the FEA.

The EL spectra of the light emitters before and after transfer onto PET (driven at 1 mA) is shown in Fig. 4a. The 425-nm peak EL emission did not show a measurable shift after integration onto the PET, suggesting that the release of the NWs from the sapphire substrate did not induce additional intrinsic stress on the NW structures.¹⁹ A measurable increase in intensity under flat conditions was observed after the PET integration and is attributed to enhanced reflectivity from the Ag n-contact bonding layer between the n-GaN and the PET. In this “flat” orientation, the cylinder structures act as a waveguide to direct light downward toward the metal contact that is reflected back toward the surface. While the bending did not affect the electrical and peak emission wavelength, the light intensity of the EL was observed to change during mechanical bending of the substrate (Fig. 4a) in the “concave-up” configuration; surprisingly, the intensity was found to increase with decreasing substrate radii of curvature.

DISCUSSION

To further understand the effect of this behavior on the LED light emission, a finite-difference time-domain (FDTD) model was used

to simulate the diode EL intensity change as a function of the substrate bending. The FEA mechanical bending model, first used to predict the induced mechanical strain during bending (Fig. 1), was also applied to determine the NW displacement, relative to each other, as a function of the radius of curvature for the substrate. The simulated displacements calculated from Fig. 4b were used to determine the tilt angles of the LEDs at $R = 38\text{ mm}$. The effect of different R values were calculated to determine the tilt of the NW structure during bending, and the displacement of the NWs in the x - and y -directions was calculated and referenced to the original position of the rods (inset Fig. 4b). The calculated tilt angles (up to 0.3° along the substrate edge) are presented in Supplementary Fig. 2.

Using the calculated tilt angles, a network of 121 NW LEDs (within a 11×11 NW array) on a GaN buffer layer having an n-contact Ag adhesive layer, at a wavelength range between 420 and 430 nm, was simulated (Supplementary Fig. 3). The simulation criteria and equations are presented in the Supplementary Discussion. Figure 5a shows the calculated near-field light intensity change of the LEDs, before and after transfer onto the PET and as a function of bending for different radii of curvature. The simulation and the experimental data show a similar trend of enhanced light extraction, due to the substrate bending. The predicted and observed improvement in light output for smaller bending radii represents an interesting and unexpected light-output enhancement regime for flexible photonic device operation. To understand this phenomenon further, the light intensity profile, collected from the topside of the NW LEDs, was investigated for (a) LED structures before transfer, (b) LEDs integrated with the silver adhesive onto PET, and (c) structure (d) with the PET having a bending radii of 38 mm (Fig. 5b–d, respectively). Initially, the increased light output after integration onto the PET (Fig. 5c) is due mainly to the increased reflectivity from the silver bonding layer used to attach the NW structures onto the PET. The measured light output also showed a similar but slightly lower increase in the EL; the difference is due in part to the nonideal optical reflection of the adhesive and the nonoptimized electrical contact of the Ag junction. The FDTD results suggest that light collection from the curved substrate is related to reducing the distance between the tips of adjacent LEDs, creating increased light integration over a smaller area away from the substrate surface. The highest light intensity was predicted to be from the NW devices on a substrate with a concave-up orientation (Fig. 5c). This geometry provides a higher effective density of light-emitting quantum dots as the tips move closer to each other during bending along with increased electromagnetic coupling between the light emitters (Supplementary Information). The higher light-emission intensity is a result of the constructive phase interference between emitted and downward reflected light for an array of cylindrical LED structures. The broader emission peaks of the experimental EL spectrum shown in Fig. 4a compared with the simulations may be due to a slight nonuniformity in the diameter of the fabricated LED devices. Combining the results from the FEA and FDTD analysis provides persuasive support for implementing NW LEDs for optimizing photonic devices using flexible platforms. This approach may be used for a broad range of applications, from flexible displays to conformal solid-state lighting, which require high brightness without additional energy consumption while maintaining uniform emission wavelengths.

The simulated and experimental findings show that substrate bending provides a means to mechanically manipulate NW LED structures that enhances their light output compared to planar device counterparts. Peak emission wavelengths remain constant during applied mechanical bending of the substrate due to the predicted small in-plane strain within the rod structure. The mechanical bending of the flexible substrate in the concave-up direction increases the light-extraction efficiency as a function of the substrate radius of curvature without introducing a shift in the

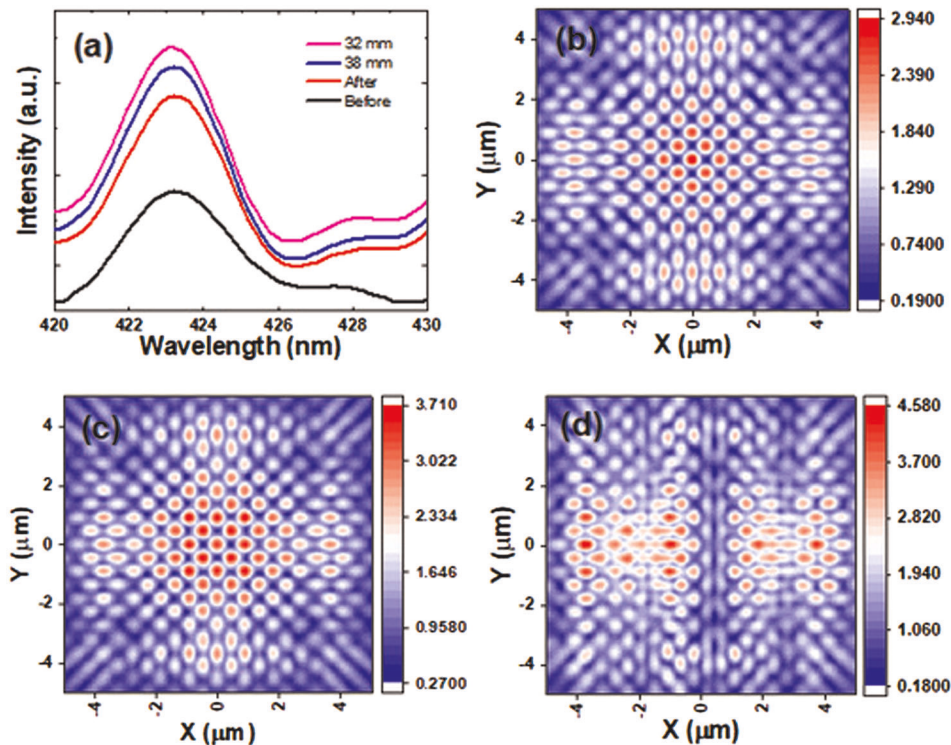


Fig. 5 **a** 3D-FDTD-simulated light-extraction efficiency for NW LEDs on different curved surfaces. The light intensity emitted from the top side of **a** freestanding NW LED device and **c** after bonding to the PET substrate using the reflective Ag adhesive. **d** The light intensity for NW LEDs on a flexible PET substrate having a 38-mm radius of curvature

peak emission wavelength. These findings add new insight to the implementation of flexible photonic structures to achieve higher light output through mechanical manipulation, providing a novel approach for realizing flexible GaN-based NW LED devices that have increased functionality and improved performance.

METHODS

Modeling and simulation

The LED structures were modeled using the commercially available FEA simulation tool, COMSOL Multiphysics. To mimic an applied bending stress on the PET substrate, a bending moment, M , applied along the ends of the substrate, was determined using the Stoney equation ($M = \frac{Ed^3w}{12R}$) for various radii of curvature, R , where d and w are the substrate thickness and width, respectively, and E is the elastic moduli.²⁰ All materials properties were assumed to be linearly elastic and temperature independent with an initial zero-bending stress. A relative tolerance of 0.001 was used for solving stationary equations with higher accuracy.

The 3D-FDTD calculations were performed using the commercial software tool, Lumerical. Perfectly match layer (PML) boundary conditions were employed to calculate the light-extraction efficiency based on integrating the Poynting vector over time along the NW surface. To increase the accuracy of the calculations, the PML attenuation factor (σ) and auxiliary attenuation factor (κ) were set to 0.25 and 2, respectively. To have meaningful results, the electromagnetic field should not change significantly from one mesh grid to another one. Accordingly, a minimum mesh step of 0.25 nm and time step of 0.0326 fs were used in all simulations. The light-emission properties were modeled as dipole sources having a wavelength range between 420 and 430 nm. The region of the NW below the active region was also considered as a photonic waveguide, providing two-dimensional light confinement along the transverse direction in the longitudinal z -direction along the length of the NW,²¹ assuming matched layer-boundary conditions along the sidewalls of the NW. A network of 121 NW LEDs (within a 11×11 array) on a GaN buffer layer was integrated with the n-contact silver-bonding layer shown in Supplementary Fig. 3.

Materials and device processing

The GaN dot-in-rod (NW) LED structures were fabricated using selective-area growth in a Veeco GENxplor radio frequency plasma-assisted molecular-beam epitaxy system. The GaN dot-in-rod LED heterostructure consists of ~ 450 nm GaN:Si, five InGaN (4 nm)/GaN (8 nm) quantum dots in the active region, and ~ 200 nm GaN:Mg segment. The growth conditions of GaN:Si segment included a substrate temperature of 990 °C and a Ga beam equivalent pressure of 2.8×10^{-7} Torr. For the growth of the InGaN/GaN quantum-dot active region, the substrate temperature was reduced to 760 °C, and the In and Ga beam equivalent pressures were 2.0×10^{-7} and 8.0×10^{-9} Torr, respectively. The GaN:Mg segment was grown at a substrate temperature of ~ 975 °C, a Ga beam equivalent pressure of 2.8×10^{-7} Torr, and a Mg beam equivalent pressure of 2.6×10^{-9} Torr. The growth temperature was referenced to a thermocouple reading at the backside of the sapphire substrate. The photoluminescence (PL) emission of such NW LED heterostructure exhibits a dominant peak with the linewidth of ~ 20 nm at ~ 427 nm that originates from the emission of InGaN quantum dots and a relatively weak peak at ~ 365 nm from emission of the GaN (Supplementary Fig. 4). In order to planarize the surface and passivate the NW sidewalls, a thin (~ 1 μm) polyimide (PI) film (from HD Microsystem, PI 2610) was spin-coated at 3000 rpm for 30 s followed by baking at 350 °C in a nitrogen oven for 30 min. A reactive oxygen etching was used to remove the PI to expose the top surface of the p-GaN segment of the NWs. Ni (6 nm)/Au (6 nm) metal layers were then deposited on p-GaN top surface and polyimide in the regions of NW arrays by photolithography and e-beam evaporation followed by rapid thermal annealing at 500 °C. A 100-nm ITO layer was deposited and annealed in vacuum to serve as a current spreading contact layer. In order to obtain uniform current injection, Ni (20 nm)/Au (100 nm) metal grids were deposited on the ITO layer using e-beam evaporation. A Ti (20 nm)/Au (100 nm) metal layer was employed as an ohmic contact to the n-GaN substrate.

LLO process

GaN NW LEDs were bonded onto a silicon wafer using Crystallbond 509-3 mounting adhesive. Following the bonding process, a 266-nm Nd:YAG laser with a power density of 900 mJ/cm² was raster scanned at 4 Hz through the transparent sapphire to decompose the GaN at the GaN/

sapphire interface. The spot size of the laser beam was $140\ \mu\text{m} \times 25\ \mu\text{m}$ and was rastered across a sample area of $1\ \text{cm} \times 1\ \text{cm}$. A thin layer of *high-performance* silver paste from Ted Pella (dispersed in an inorganic silicate aqueous solution) was used to attach the exposed n-side of the GaN devices onto the flexible PET substrate. This structure was immersed into a hot acetone bath to selectively dissolve the Crystallbond adhesive layer and release the silicon carrier substrate. The samples were then sequentially immersed in fresh acetone and alcohol baths for 5 min each to wash out any adhesive residue from the topside of the NW LEDs and metal contacts. The “double-transfer” process was completed by drying the samples with nitrogen gas.

Device characterization

PL measurements were carried out at room temperature using a 325-nm He–Cd laser excitation source (IK Series, KIMMON KOHA). The incident beam was focused on the sample surface through a $15\times$ objective lens. The PL light from the sample was resolved by a high-resolution spectrometer (iHR550, HORIBA) with 1200 g/mm grating and detected by a photomultiplier tube. A long-pass filter ($>355\ \text{nm}$) was placed in front of the entrance of the spectrometer.

The NW LED I–V characteristics were measured before and after integration onto the PET substrates using a Micromanipulator 7000 probe station and a Keithley 6430 parameter analyzer. The EL measurements of the devices on a curved PET substrate were accomplished, using the same instrumentation with the samples attached to curved substrate holders made from machined aluminum. The samples were taped onto the holders using adhesive Kapton® tape. The devices were then probed directly in a curved orientation of different radii of curvature.

The EL measurements were accomplished using an Ocean Optics SB2000+UV-VIS spectrophotometer with a Sony ILX511B 2048 element linear silicon CCD array with an optical resolution of 1.5 nm (full width at half maximum). The devices were attached to the substrate holders and were then probed directly in flat and curved orientations of different radii of curvature.

Structural characterization

The SEM images were taken using a JSM-7200F JEOL microscope system. The experiments were performed with 0° , 90° , and 45° angle sample holders to observe the device cross section. An accelerating voltage of 10 kV was used for imaging. The AFM scans were performed on a Veeco Bruker DI Dimension 3100 systems using a Si probe tip. The scan was operated under tapping mode over a scan area of $100\ \mu\text{m}^2$ with a scan rate of 1 Hz.

DATA AVAILABILITY

The authors declare that [the/all other] data supporting the findings of this study are available within the paper [and its Supplementary Information files].

ACKNOWLEDGEMENTS

This work was performed using the facilities in the Giga-to-Nanoelectronics Center at the University of Waterloo. The authors acknowledge support from the Natural Sciences and Engineering Research Council Strategic Partnership Grant (STPGP-463397-2014), the Canadian Microelectronics Corporation, and MW Canada Ltd. The authors acknowledge the helpful technical discussions of the Prof. Michael Reimer from the University of Waterloo.

AUTHOR CONTRIBUTIONS

M.A. and W.S.W. designed the experimental investigation, and R.W. and Y.-H.R. contributed to the GaN dot-in-wire LED fabrication and part of the analysis of the LED device characterization. M.A. and P.G. performed the FEA analysis, while M.A. executed experimental work, analysis of the results, and wrote the paper. W.S.W. and Z.M. contributed to the analysis and writing of the paper. All authors reviewed the paper.

ADDITIONAL INFORMATION

Supplementary information accompanies the paper on the *npj Flexible Electronics* website (<https://doi.org/10.1038/s41528-019-0059-z>).

Competing interests: The authors declare no competing interests.

Publisher's note: Springer Nature remains neutral with regard to jurisdictional claims in published maps and institutional affiliations.

REFERENCES

- Nguyen, H. P. T. et al. Breaking the carrier injection bottleneck of phosphor-free nanowire white light-emitting diodes. *Nano Lett.* **13**, 5437–5442 (2013).
- Li, K. H., Liu, X., Wang, Q., Zhao, S. & Mi, Z. Ultralow-threshold electrically injected AlGaIn nanowire ultraviolet lasers on Si operating at low temperature. *Nat. Nanotechnol.* **10**, 140–144 (2015).
- Djavid, M. & Mi, Z. Enhancing the light extraction efficiency of AlGaIn deep ultraviolet light emitting diodes by using nanowire structures. *Appl. Phys. Lett.* **108**, 1–5 (2016).
- Grzela, G. et al. Nanowire antenna emission. *Nano Lett.* **12**, 5481–5486 (2012).
- Van Dam, D. et al. Directional and polarized emission from nanowire arrays. *Nano Lett.* **15**, 4557–4563 (2015).
- Diedenhofen, S. L. et al. Controlling the directional emission of light by periodic arrays of heterostructured semiconductor nanowires. *ACS Nano* **5**, 5830–5837 (2011).
- Dai, X. et al. Flexible light-emitting diodes based on vertical nitride nanowires. *Nano Lett.* **15**, 6958–6964 (2015).
- Shervin, S. et al. Bendable III-N visible light-emitting diodes beyond mechanical flexibility: theoretical study on quantum efficiency improvement and color tunability by external strain. *ACS Photonics* **3**, 486–493 (2016).
- Tabares, G. et al. Impact of the bending on the electroluminescence of flexible InGaIn/GaN light-emitting diodes. *IEEE Photonics Technol. Lett.* **28**, 1661–1664 (2016).
- Hong, R.-H., Tien, C.-H., Chuang, S.-H., Liu, K.-C. & Wu, D.-S. External stress effects on the optical and electrical properties of flexible InGaIn-based green light-emitting diodes. *Opt. Express* **23**, 31334 (2015).
- Tawfik, W. Z., Hyun, G. Y., Ryu, S. W., Ha, J. S. & Lee, J. K. Piezoelectric field in highly stressed GaN-based LED on Si (1 1 1) substrate. *Opt. Mater.* **55**, 17–21 (2016).
- Pathirane, M. K. & Wong, W. S. Optical and electrical characteristics of hybrid ZnO nanowire/a-Si:H solar cells on flexible substrates under mechanical bending. *Small* **12**, 2554–2558 (2016).
- Wong, W. S. et al. In_xGa_{1-x}N light emitting diodes on Si substrates fabricated by Pd – In metal bonding and laser lift-off. *Appl. Phys. Lett.* **77**, 2822–2824 (2000).
- Wong, W. S., Sands, T. & Cheung, N. W. Damage-free separation of GaN thin films from sapphire substrates. *Appl. Phys. Lett.* **72**, 599–601 (1998).
- Wong, W. S. et al. Fabrication of thin-film InGaIn light-emitting diode membranes by laser lift-off. *Appl. Phys. Lett.* **75**, 1360 (1999).
- Kim, T. II et al. High-efficiency, microscale GaN light-emitting diodes and their thermal properties on unusual substrates. *Small* **8**, 1643–1649 (2012).
- Kneissl, M. et al. Continuous-wave operation of InGaIn multiple quantum well laser/diodes on copper substrates obtained by laser lift-off. *IEEE J. Sel. Top. Quantum Electron.* **7**, 188–191 (2000).
- Matienco, L. J., Das, R. N. & Egitto, F. D. Electrically conductive adhesives for electronic packaging and assembly applications. *J. Adhes. Sci. Technol.* **22**, 853–869 (2008).
- Chun, J. et al. Transfer of GaN LEDs from sapphire to flexible substrates by laser lift-off and contact printing. *IEEE Photonics Technol. Lett.* **24**, 2115–2118 (2012).
- Feng, X., Huang, Y. & Rosakis, A. J. On the Stoney formula for a thin film/substrate system with nonuniform substrate thickness. *J. Appl. Mech.* **74**, 1276 (2007).
- Reimer, M. E. et al. Bright single-photon sources in bottom-up tailored nanowires. *Nat. Commun.* **3**, 737 (2012).



Open Access This article is licensed under a Creative Commons

Attribution 4.0 International License, which permits use, sharing, adaptation, distribution and reproduction in any medium or format, as long as you give appropriate credit to the original author(s) and the source, provide a link to the Creative Commons license, and indicate if changes were made. The images or other third party material in this article are included in the article's Creative Commons license, unless indicated otherwise in a credit line to the material. If material is not included in the article's Creative Commons license and your intended use is not permitted by statutory regulation or exceeds the permitted use, you will need to obtain permission directly from the copyright holder. To view a copy of this license, visit <http://creativecommons.org/licenses/by/4.0/>.

© The Author(s) 2019